Review Article

Adrenal imaging (Part 1): Imaging techniques and primary cortical lesions

Ananya Panda, Chandan J. Das, Ekta Dhamija, Rakesh Kumar[1], A. K. Gupta

Departments of Radiology and [1]Nuclear Medicine, All India Institute of Medical Sciences, Ansari Nagar, New Delhi, India

ABSTRACT

Adrenal glands can be affected by a variety of lesions. Adrenal lesions can either be primary, of adrenal origin, or secondary to other pathologies. Primary adrenal lesions can further be either of cortical or medullary origin. Functioning adrenal lesions can also give clues to the histologic diagnosis and direct workup. Over the years, various imaging techniques have been developed that have increased diagnostic accuracy and helped in better characterization of adrenal lesions non-invasively. In the first part of the two part series, we review adrenal imaging techniques and adrenal cortical tumors such as adenomas, adrenocortical tumors, adrenal hyperplasia and oncocytomas.

Key words: Adrenal adenoma, adrenal cancer, adrenal imaging, adrenocortical carcinoma

Introduction

The adrenal glands play a vital role in the physiological regulation of the human body. Belying their small size, they can be affected by a variety of benign and malignant lesions in both children and adults. The classification of adrenal lesions can be complex reflecting the histologic complexity of adrenal glands. Adrenal lesions can be broadly divided into primary or secondary lesions. Primary adrenal lesions, that is, arising from adrenal gland itself can be either of cortical or medullary origin. Furthermore, primary adrenal lesions can be either functioning or non-functioning, with functional adrenal lesions being an important cause of referral to endocrinology department.[1] The various adrenal lesions have been enumerated in Table 1.

Adrenal lesions can also be classified on basis of laterality, that is, unilateral or bilateral. Bilateral lesions can also manifest with syndromes of either hormone overproduction (Conn's syndrome due to bilateral adrenal hyperplasia, hypertension due to bilateral pheochromocytomas) or hormone deficiency (Addison's syndrome due to granulomatoses, hemorrhage, lymphoma).

Radiology plays an essential role in imaging of adrenal lesions and is complementary to functional imaging and hormonal evaluation in workup of functioning tumors.[2] With advances in radiologic techniques, imaging can also obviate invasive sampling in many cases.

Thus, the two-part reviews provide an insight into radiological techniques used in imaging of adrenal glands and radiologic appearances of various adrenal lesions. The first part describes the adrenal imaging techniques, normal appearances of adrenal glands and primary adrenal tumors of cortical origin while the second part deals with primary adrenal medullary tumors, secondary adrenal lesions, bilateral adrenal lesions, adrenal incidentalomas and concludes by summarizing the current approach to adrenal lesions.

Access this article online	
Quick Response Code:	Website: www.ijem.in
	DOI: 10.4103/2230-8210.146858

Imaging modalities and normal imaging appearances

The role of imaging in adrenal lesions is essentially to differentiate benign and malignant lesions, metastatic from non-metastatic lesions and provide definitive diagnosis

Corresponding Author: Dr. Chandan J. Das, Department of Radiology, All India Institute of Medical Sciences, Ansari Nagar, New Delhi - 110 029, India. E-mail: docchandan17@gmail.com

wherever possible to obviate further invasive testing. Fortunately at present, with a wide array of imaging techniques at disposal, anatomic imaging can give the definitive diagnosis in most cases, thereby eliminating the need for further testing. Functional imaging however plays a greater role in imaging medullary tumors such as pheochromocytomas and occasionally in neuroblastomas.

Ultrasonography (USG) is a readily available technique for evaluation of abdominal pathologies. Though the visualization of retroperitoneal structures like adrenals is difficult on USG, it still has a role in incidentally detecting adrenal masses, in monitoring the changes during treatment of already established pathology and enables visualization of other abdominal organs at the same setting without any risk of radiation exposure and is cost effective.[3,4] USG shows adrenal glands quite accurately in infants and children [Figure 1] as compared to adults where they may be obscured due to bowel gas and obesity. On USG, if no mass is seen with or without visualization of normal adrenals, it is considered to be specific for the absence of malignancy.

Contrast-enhanced ultrasonography: Friedrich-Rust *et al*.[5] have studied the efficacy of contrast enhanced USG (CEUS) in evaluation of adrenal masses using phospholipid stabilized microbubbles filled with sulfur hexafluoride (SonoVue) [Figure 1]. Arterial enhancement with rapid washout is seen in the non-adenomatous masses. They found efficacy of CEUS to be comparable to CT and MRI for detection of adrenal malignancy with sensitivity of 100% and specificity of 82%. Diameter greater than 4 cm was found to have 90% sensitivity and 24% specificity in the detection of adrenocortical carcinoma (ACC). The study recommended opting for CEUS for analysis of adrenal masses as initial radiological examination as it would reduce the radiation exposure occurring in multiphase computed tomography (MPCT) and significantly reduces the cost and time required for MRI.[5]

Computed tomography (CT) is undoubtedly the mainstay of adrenal imaging. But with the widespread use of multidetector CT, there has also been an increase in detection of incidental adrenal nodules/incidentalomas.[6,7] Normal adrenal glands are seen as inverted V- or Y-shaped structures lying anterosuperior to the kidneys in the retroperitoneum [Figure 2]. The glands are readily identified owing to the presence of abundant retroperitoneal fat in most patients. The two limbs are thinner as compared to

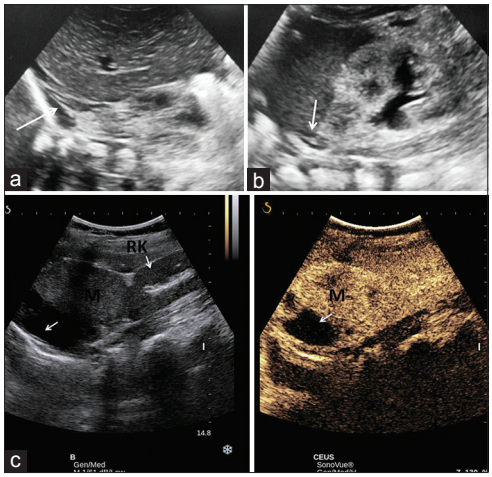

Figure 1: Normal ultrasound appearances. Ultrasound of a 3-day old infant showing V-shaped right adrenal (a) in suprarenal location formed by its two hypoechoic limbs. Hypoechoic limb of left adrenal is well visualized in left suprarenal location (b). Contrast enhanced ultrasound appearance. Right half of the image showing a large suprarenal mass (M) separate from right kidney (RK) with areas of necrosis (arrow). Left half of the image showing avid enhancement of the suprarenal mass (M) like the kidney with nonenhancing necrotic area (arrow) after intravenous injection of ultrasound contrast agent perflurocarbon (SonoVue) (c)

Table 1: Comprehensive classification of adrenal lesions based on etiology, cell of origin and hormone secreting status

Adrenal lesions	Histologic origin	Benign	Malignant	Hormone excess	Syndrome
Primary	Cortical	Adenoma	Adrenocortical Carcinoma	Aldosterone (zona glomerulosa) Glucocorticoids (zona fasciculata) Sex hormones (zona reticulata)	Conn's syndrome Cushing's syndrome Virilizing syndromes
		Adrenal hyperplasia		Aldosterone (Zona glomerulosa) Sex hormones (Zona reticulata)	Conn's syndrome Virilizing syndromes
		Oncocytoma	Malignant oncocytoma	Non-functioning	None
	Medullary	Pheochromocytoma	Malignant pheochromocytoma	Catecholamines	Symptoms of excess catecholamine such as palpitations, tachycardia, hypertension
		Ganglioneuroma	Neuroblastoma Ganglioneuroblastoma		
Secondary	No specific histologic origin	Myelolipoma Cysts Lipoma Hemorrhage	Metastases Lymphoma	None	None
Other entities	Any cell origin/ Either primary or secondary	Incidentalomas Collision tumors (adenoma+myelolipoma)	Collision tumors (adenoma+metastases)	None	None

the apex where two limbs join. Mean thickness of gland is 5-6 mm with maximum width of 10 mm and approximate length is 2-4 cm in one section of CT.[4,8,9] Paucity of retroperitoneal fat may render visualization of adrenals difficult due to overlap of surrounding structures.

Both unenhanced CT and multiphase contrast-enhanced CT have role in adrenal imaging. On unenhanced CT, the presence of macroscopic fat confirms diagnosis of a benign myelolipoma while an attenuation of less than 10 Hounsfield units (HU) suggests diagnosis of benign adrenal adenoma and further testing is not required [Figure 3].

Another adjunct to unenhanced CT is CT histogram analysis using software incorporated in the newer CT machines. It plots the attenuation value of each pixel in region of interest (ROI) with respect to its frequency. Number of negative pixels (i.e. less than 0 HU) in ROI corresponds to amount of lipid content. Hence, more the number of negative pixels, more the lipid content within. It has been noted that value of <10 HU on unenhanced CT or >10% negative pixel content on histogram identifies 91% adenomas correctly as compared to 66% detection when unenhanced CT is used alone.[10]

Multiphase CT (MPCT) protocols in adrenal imaging is based on the fact that while both adenoma and malignant lesions show rapid contrast enhancement, adenomas show rapid washout of contrast as well while malignant masses show slower washout. The CT protocol comprises of baseline non-contrast scan through adrenal glands followed by a contrast-enhanced scan at portal venous phase (60-70 seconds) followed by delayed scan at 15 minutes. From these scans, absolute percentage washout (APW) (Attenuation in contrast-delayed scan/attenuation in contrast-non contrast × 100) and relative percentage washout (RPW) (attenuation in contrast-delayed/attenuation in contrast scan × 100) can be calculated which helps in differentiating benign adenomas from other adrenal lesions. It is important to place ROI for estimation of attenuation value such that approximately one-half to two-third of the adrenal surface area is covered and care should be taken to exclude the necrotic component.[7]

Magnetic resonance imaging (MRI) has very specific indications in adrenal imaging. While normal adrenal has low to intermediate signal intensity on both T1- and T2-weighted sequence [Figure 4], MRI does not offer additional spatial resolution and is chiefly used as an alternative to CT when contrast-enhanced CT is contraindicated. Chemical shift imaging (CSI) is a non-contrast MRI technique that can be used for diagnosis

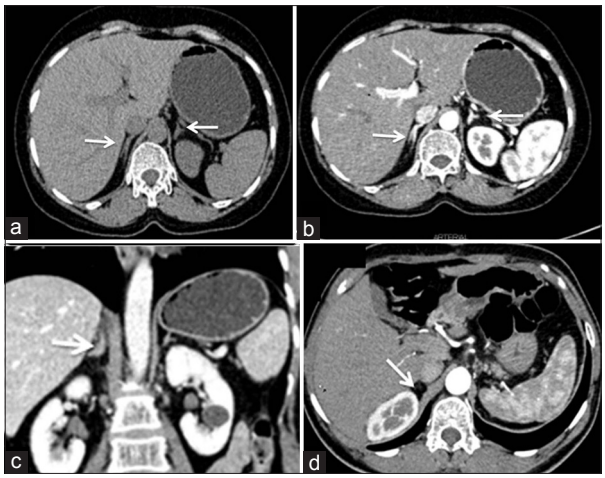

Figure 2: Normal CT appearance. CT axial section: (a) V-shaped right adrenal and Y-shaped left adrenal gland in the retroperitoneum; seen well due to abundant retroperitoneal fat. (b) Predominantly arterial phase scan showing uniform and homogeneous enhancement of both adrenals. (c) Coronal reformatted images showing suprarenal location of normal adrenal glands (white arrows in a,b,c). Post adrenalectomy CT (d) showing absent adrenal limb (arrow) behind IVC

Figure 3: Utility of unenhanced CT. Unenhanced axial CT done for a patient with abdominal pain. A well-defined lesion in left adrenal has macroscopic fat (–27 HU) confirming benign nature of the mass

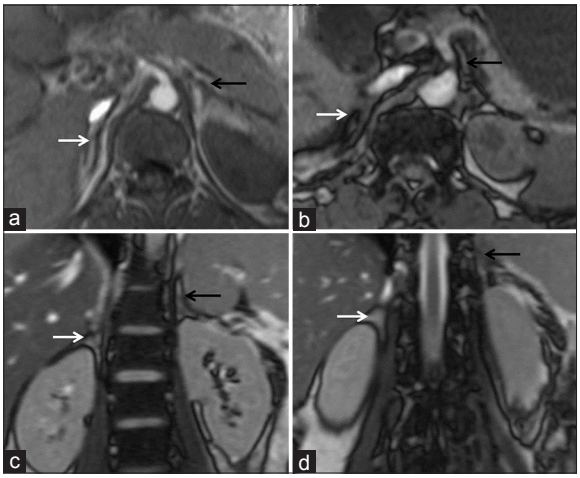

Figure 4: Normal MRI appearance Axial T1 weighted in phase (a) and opposed phase (b) imagesand coronal (c, d) images demonstrating normal adrenal glands as V- and Y-shaped structures with intermediate signal intensity on both sequences

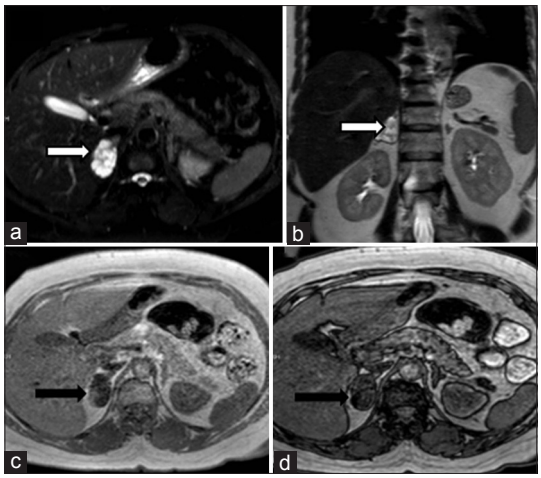

Figure 5: Chemical shift imaging in adenoma. Lady on follow up for incidentally detected asymptomatic right adrenal mass. Recent MRI showing well-defined hyperintense mass on T2-weighted images with hypointense foci within [White arrow in axial and coronal images, (a) and (b)]. The mass is hypointense on in-phase T1 sequence (c) with subtle hyperintense focus along the lateral margin which shows loss of signal on T1 out-of-phase sequence. The mass is diagnosed to be non-functioning right adrenal adenoma (lipid poor) which is stable over 2 years

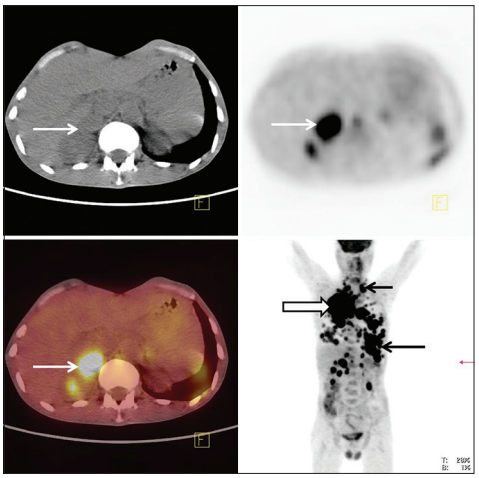

Figure 6: FDG-PET/CT scan for detection of metastases. FDG-PET/CT images of patient with right lung cancer (block arrow) showing avid FDG uptake by right adrenal mass (white arrow). There are multiple other areas of FDG uptake in on PET image (black arrows) consistent with diffuse metastatic disease

of adenoma when CT is contraindicated or washout values are equivocal. It is based on the principle that fat has a lower precession resonant frequency than water in the presence of an externally applied magnetic field. Thus, during T1-weighted gradient echo sequence (GRE), if fat and water are in the same voxel (i.e. microscopic fat) as seen in adenomas, the signal of lipid and water gets summated in the in-phase image but gets nulled out during out-phase sequence[11,12] [Figure 5]. This drop in signal intensity in CSI has sensitivity (81-100%) and specificity (94-100%) similar to unenhanced CT densitometry for the differentiation of incidental adrenal lesions.[2] While for lipid-rich adenomas, there is effectively no difference between CT and MRI, CSI might be superior when evaluating lipid-poor adenomas.[7,13]

MRI can also be used to confirm macroscopic fat in myelolipoma which shows drop in signal in the fat-suppressed sequence. Drawback remains in the case of ACC, pheochromocytoma, and clear cell renal cell cancer metastasis, which may also have macroscopic lipid content.[7,14-16]

Positron emission tomography (PET) and PET-CT combine the utility of HU measurements on unenhanced CT along with functional activity. With current high-resolution scanners, even lesions as small as 5 mm can be assessed.[13] Both qualitative assessment (comparison of activity with liver) and quantitative assessment can differentiate benign and malignant adrenal lesions with high sensitivity (98-100%) and specificity (93-98%).[17-19] FDG-PET can also help in response assessment in lymphomas and be used in disease staging by detecting total disease burden in both primary ACC, neuroblastomas and secondary metastases[20] [Figure 6]. FDG-PET/CT is also useful in detecting methyl-iodo-benzyl-guanimidine (MIBG)-negative pheochromocytomas as described by Shulkin *et al*.[21] However, pitfalls include 5% false positive results due to uptake seen in functioning adenomas and inflammatory conditions such as sarcoidosis, tuberculosis or in adrenal cortical hyperplasia and false-negative results as metastases from primary low FDG avid tumors like bronchioalveolar carcinoma and carcinoid do not show significant FDG uptake.[22]

Adrenal cortical tumors

Adrenal adenoma

The incidence of adenoma increases with age, being 0.14% in age group of 20-29 years increasing to 7% in patients more than 70 years.[6,7,23] The adenomas can be functioning or non-functioning; latter being commonly encountered as an incidental lesion. Clinical presentation depends on the product secreted by the adenoma-Cushing's syndrome in cortisol-secreting tumors, Conn's syndrome with hyperaldosteronemia and adrenal virilization due to androgen-secretion.[1]

On imaging, adenoma is usually small in size (<1 cm); however, size may range from 1 to 5 cm. They are well-defined, homogeneous masses with smooth contours. On unenhanced CT, attenuation less than 10 HU is suggestive of adenomas but varies from –2 HU (lipid-rich) to 60 HU (lipid-poor adenomas) depending on amount of intracellular/microscopic fat. Since only 70% of the adenomas are lipid-rich; MRI can help in detecting microscopic fat in lipid poor adenomas by showing signal dropout on opposed phase CSI[24-26] [Figure 5 and 7]. On contrast enhanced CT,

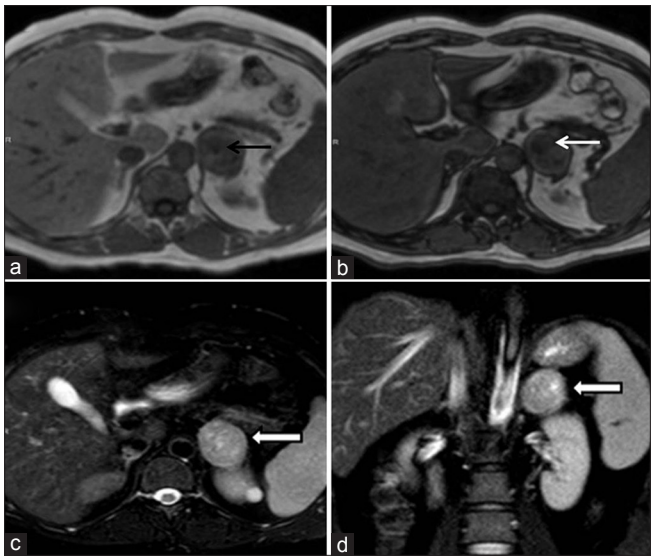

Figure 7: MRI of adenoma. Incidentally detected left adrenal mass in a boy during evaluation for abdominal pain. The mass is iso to hypointense on T1-weighted in-phase image (bold arrow in a) and showing signal drop in out-phase sequence (thin white arrow in b). The mass has hyperintense signal on T2 WI (white arrow in c and d)

adenomas show rapid enhancement and washout with APW >60% and RPW >40%.[25]

Anatomic imaging cannot differentiate functioning from non-functioning adenomas; however; it has been postulated that functioning tumors cause suppression of release of ACTH (adrenocorticotrophin hormone) which causes atrophy of contralateral adrenal gland.[4]

Adrenocortical carcinoma

ACC is overall a rare tumor but represents the most common malignant adrenal tumor in a patient without an underlying malignancy. It has a bimodal age of presentation, affecting children in their first decade and adults in their fourth and fifth decades. In children, ACC are more likely to be smaller in size and functioning thus presenting early with endocrine dysfunction. In adults, tumors are larger in size, non-functioning and present late with abdominal pain and lump, local invasion and distant metastases.[13] Hereditary ACCs have been described in various familial syndromes like Li-Fraumeni syndrome, Beckwith-Wiedemann syndrome, Carney's complex, familial adenomatoses polyposis coli and multiple endocrine neoplasia (MEN)-type 1.

On CT, ACCs usually present as large (more than 6 cm) and heterogeneous lesions with necrosis and hemorrhage replacing the entire adrenal gland. Enhancement can be peripheral or rim-like with central necrosis and absent contrast washout. Occasionally, they can be less than 5 cm and well-defined in children, thereby mimicking adenomas. The RPW and APW are typically less than

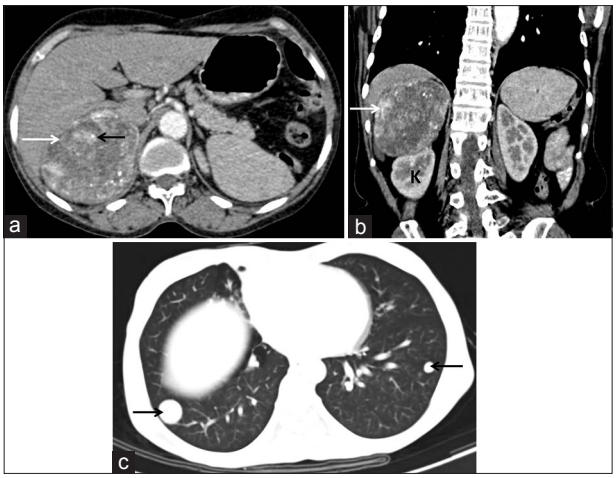

Figure 8: Adrenocortical carcinoma with lung metastases. Axial CT section (a) and coronal reformatted (b) images showing a heterogeneously enhancing, necrotic right suprarenal mass (white arrows) with intralesional calcifications (black arrow, a). The mass is displacing the right kidney (K) inferiorly. Lung window axial CT image (c) showing metastatic nodules in lower lobes of both lungs (arrows, c)

40% and 60% respectively thus differentiating from benign adenomas[27] [Figure 8]. Calcifications can be seen in up to 30% of these tumors, differentiating them from adenomas which do not show calcifications and pheochromocytomas which show calcifications in only 10%.[25] CT also shows local invasion and contiguous tumor extension into liver, pancreas, kidney and diaphragm. Similarly invasion of inferior cava invasion, if seen in an adrenal mass, is typical for ACC. Metastases can be seen in up to 30% of cases to regional lymph nodes, liver, lungs and bones [Figures 8 and 9]. Surgical resection, either curative or debulking is the treatment of choice for all ACCs irrespective of tumor size and local invasion. However, peritoneal carcinomatosis has also been reported in ACCs and is attributed to tumor spill and incomplete resection during surgery, both by laparoscopic and open techniques[28-30] [Figure 10].

On MRI, ACCs have heterogeneous signal intensity on T1 and T2 images, with T1 hyperintensity due to hemorrhage and T2 hyperintensity due to necrosis [Figure 11]. MRI can also better depict the IVC invasion and extent of tumor thrombus.[31,32]

Atypical imaging features of ACCs include the presence of intracytoplasmic fat due to cortisol precursors in hormonally active tumors causing signal drop on opposed phase CSI-MR images[33] and APW and RPW of more than 60% and 40% respectively thereby mimicking adenomas.[34] Isolated cases of macroscopic fat within the tumor mimicking myelolipoma have also been reported.[14-16] However, such imaging features are exceptions and their presence in large and heterogeneous adrenal masses should not be mislabeled as a benign adenoma or myelolipoma.

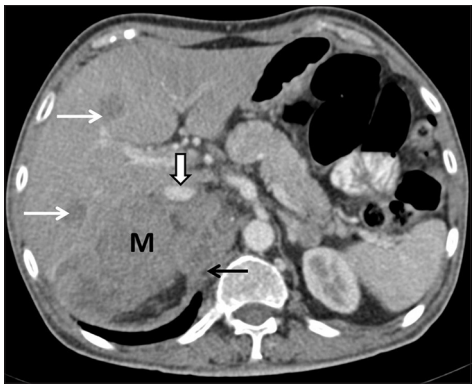

Figure 9: Adrenocortical carcinoma with liver metastases. CT axial image showing ill-defined, infiltrative right adrenal mass (M), displacing the inferior vena cava anteriorly (block arrow), invading right crus of diaphragm (black arrow) and multiple liver metastases (white arrows). There is focal loss of fat planes without any obvious infiltration of liver. The anterior displacement of inferior vena cava is consistent with an adrenal mass

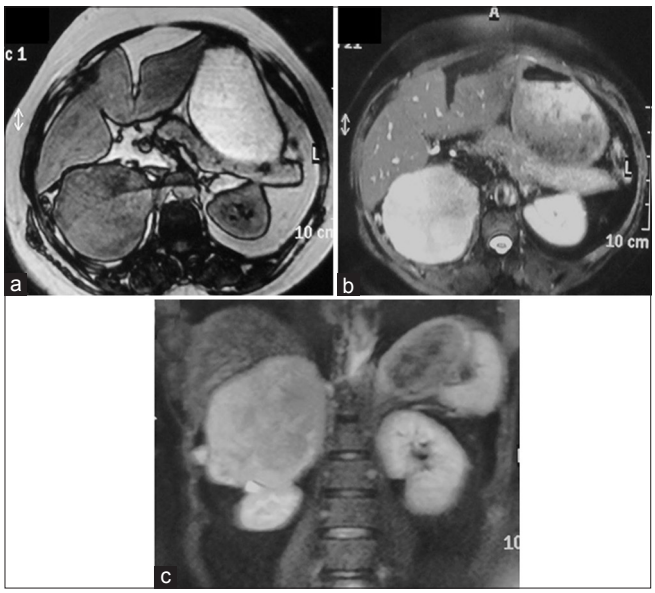

Figure 11: MR appearance of adrenocortical carcinoma. Axial T1-weighted opposed phase (a) , T2-weighted axial (b) and coronal (c) images showing a T1 hypointense and T2 hyperintense mass in the right suprarenal region displacing right kidney inferiorly. There is no obvious hepatic and renal infiltration. This MR appearance is non-specific and can also be seen in pheochromocytomas

Bilateral adrenal hyperplasia

BAH is another cause of primary aldosteronemia/Conn's syndrome or ACTH-independent Cushing's syndrome and needs to be differentiated from functioning adenoma as the management is medical in BAH while it is surgical in adenoma.[1,35] BAH can be diffuse or nodular. Diffuse AH manifests as diffuse and smooth increase in size of adrenal glands with maintained shape. Nodular hyperplasia can be identified on imaging if associated with macronodules. These appear as small hypo-to-iso-attenuating nodules on background of atrophied or normal appearing adrenal glands.[36] Diagnosis of BAH can be suggested if adrenal

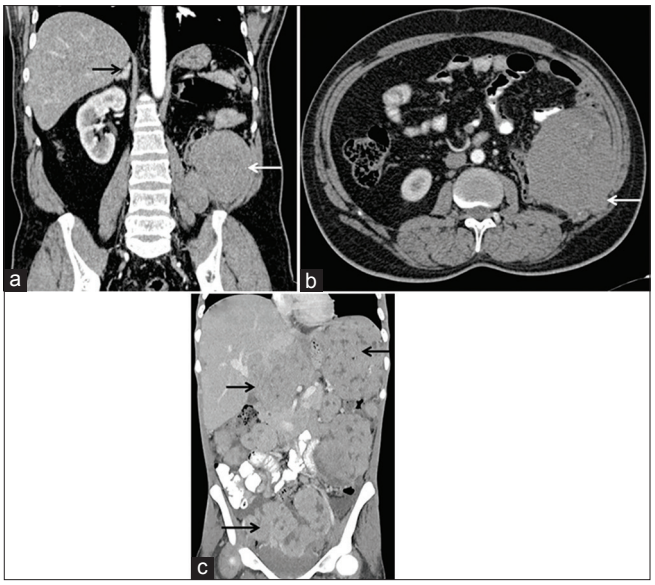

Figure 10: Recurrence of adrenocortical carcinomas. (a, b) Patient with previous history of left adrenocortical carcinoma, post left adrenalectomy and nephrectomy status. Coronal reformatted image (a) and axial CT section (b) show a locally invasive recurrent mass in the left flank region (white arrow a, b). The left adrenal and kidney are not seen, due to post-operative status while right adrenal gland is normal (black arrow, a). (c) Another patient with a prior right adrenocortical carcinoma resected laparoscopically. Coronal reformatted CT image shows tumor recurrence manifesting with multiple peritoneal deposits (black arrows) in abdomen and pelvis consistent with peritoneal carcinomatosis. (Image courtesy: Dr. Chandrashekhara SH, Assistant Professor, Department of Radiology, BRAIRCH, AIIMS, New Delhi)

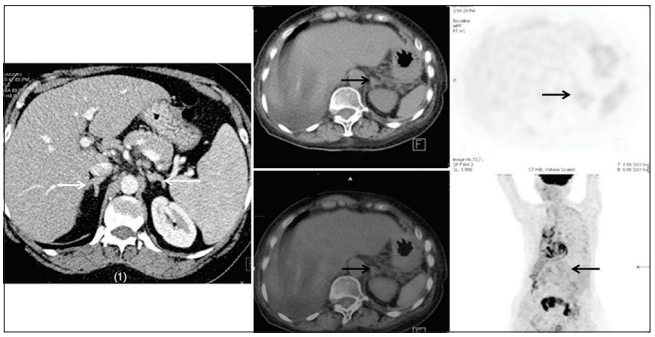

Figure 12: Adrenal hyperplasia Patient 1 is a male who is a follow-up case of primary malignancy of lung. CT done for staging revealed bilaterally symmetrical thickening of adrenals with no mass lesion in either of the glands. Note that the normal contour of the glands is maintained. Patient 2 is 5 years old girl with clinical suspicion of adrenogenital syndrome. CT showed hyperplasia of adrenals (only left adrenal seen in the image) and no uptake is seen on PET images

vein sampling shows bilateral disease and scintigraphy using cholesterol-based radionuclides shows bilateral uptake[1] [Figure 12].

Adrenal cortical oncocytomas

Adrenal oncocytic cortical tumors or adrenal oncocytomas are rare tumors and can be either benign or malignant. These can be diagnosed only on histology. However, increased detection of adrenal lesions on cross-sectional

imaging, improved awareness and retrospective reviews have led to an increase in reporting of this hitherto rare entity.[37,38] While benign tumors cannot be differentiated from lipid-poor adenomas, malignant oncocytomas mimic ACC with similar large sizes, necrosis and poor contrast washout.[37] Though oncocytomas can cause a mass effect on surrounding organs, direct organ invasion is uncommon due to the presence of fibrous capsule.[25,39] Tirkes *et al*.[37] in their retrospective review of nine oncocytomas have proposed that the absence of local organ or venous invasion even in the presence of large adrenal masses should lead to diagnostic consideration of an oncocytoma over ACC.

Conclusion

Primary adrenal tumors of either cortical or medullary origin have diverse imaging appearances. Using various imaging techniques and correlation with clinical symptoms and functional assays, definitive diagnoses can be given in most lesions. CT is currently the mainstay of imaging of primary adrenal lesions but is well complemented by MRI and functional assays whenever required. Thus, the availability of various imaging techniques has made diagnosis of primary adrenal lesions fairly straight forward.

References

1. Chaudhary V, Bano S. Anatomical and functional imaging in endocrine hypertension. Indian J Endocrinol Metab 2012;16:713-21.
2. Das CJ, Baruah MP, Baruah UM. Radiological imaging in endocrine hypertension. Indian J Endocrinol Metab 2011;15 Suppl 4:S383-8.
3. Yeh HC. Sonography of the adrenal glands: Normal glands and small masses. AJR Am J Roentgenol 1980;135:1167-77.
4. Podgórska J, Cieszanowski A, Bednarczuk T. Adrenal imaging. Endokrynol Pol 2012;63:71-81.
5. Friedrich-Rust M, Schneider G, Bohle MR, Herrmann E, Sarrazin C, Zeuzem S, *et al*. Contrast-enhanced sonography of adrenal masses: Differentiation of adenomas and nonadenomatous lesions. AJR Am J Roentgenol 2008;191:1852-60.
6. Dunnick NR, Korobkin M, Francis I. Adrenal radiology: Distinguishing benign from malignant adrenal masses. AJR Am J Roentgenol 1996;167:861-7.
7. Blake MA, Cronin CG, Boland GW. Adrenal imaging. AJR Am J Roentgenol 2010;194:1450-60.
8. Montagne JP, Kressel HY, Korobkin M, Moss AA. Computed tomography of the normal adrenal glands. AJR Am J Roentgenol 1978;130:963-6.
9. Haaga JR, Lanzieri CF. CT and MR imaging of the whole body. In: Timothy WJ, Patrick SF 2nd, editors. The Adrenal Glands. Minnesota; 2003. p. 1511-36.
10. Halefoglu AM, Bas N, Yasar A, Basak M. Differentiation of adrenal adenomas from nonadenomas using CT histogram analysis method: A prospective study. Eur J Radiol 2010;73:643-51.
11. Brateman L. Chemical shift imaging: A review. AJR Am J Roentgenol 1986;146:971-80.
12. Hood MN, Ho VB, Smirniotopoulos JG, Szumowski J. Chemical shift: The artifact and clinical tool revisited. Radiographics 1999;19:357-71.
13. Taffel M, Haji-Momenian S, Nikolaidis P, Miller FH. Adrenal imaging: A comprehensive review. Radiol Clin North Am 2012;50:219-43.
14. Egbert N, Elsayes KM, Azar S, Caoili EM. Computed tomography of adrenocortical carcinoma containing macroscopic fat. Cancer Imaging 2010;10:198-200.
15. Ferrozzi F, Bova D. CT and MR demonstration of fat within an adrenal cortical carcinoma. Abdom Imaging 1995;20:272-4.
16. Sato N, Watanabe Y, Saga T, Mitsudo K, Dohke M, Minami K. Adrenocortical adenoma containing a fat component: CT and MR image evaluation. Abdom Imaging 1995;20:489-90.
17. Metser U, Miller E, Lerman H, Lievshitz G, Avital S, Even-Sapir E. 18F-FDG-PET/CT in the evaluation of adrenal masses. J Nucl Med 2006;47:32-7.
18. Boland GW, Blake MA, Holalkere NS, Hahn PF. PET/CT for the characterization of adrenal masses in patients with cancer: Qualitative versus quantitative accuracy in 150 consecutive patients. AJR Am J Roentgenol 2009;192:956-62.
19. Jana S, Zhang T, Milstein DM, Isasi CR, Blaufox MD. FDG-PET and CT characterization of adrenal lesions in cancer patients. Eur J Nucl Med Mol Imaging 2006;33:29-35.
20. Blake MA, Prakash P, Cronin CG. PET/CT for Adrenal Assessment. Am J Roentgenol 2010;195:W91-5.
21. Shulkin BL, Koeppe RA, Francis IR, Deeb GM, Lloyd RV, Thompson NW. Pheochromocytomas that do not accumulate metaiodobenzylguanidine: Localization with PET and administration of FDG. Radiology 1993;186:711-5.
22. Chong S, Lee KS, Kim HY, Kim YK, Kim BT, Chung MJ, *et al*. Integrated PET-CT for the characterization of adrenal gland lesions in cancer patients: Diagnostic Efficacy and interpretation pitfalls. Radiographics 2006;26:1811-24.
23. Willatt JM, Francis IR. Radiologic evaluation of incidentally discovered adrenal masses. Am Fam Physician 2010;81:1361-6.
24. Krebs TL, Wagner BJ. MR imaging of the adrenal gland: Radiologic-pathologic correlation. Radiographics 1998;18:1425-40.
25. Johnson PT, Horton KM, Fishman EH. Adrenal mass imaging with multidetector CT: Pathologic conditions, pearls, and pitfalls. Radiographics 2009;29:1333-51.
26. Boland GW, Blake MA, Hahn PF, Mayo-Smith WW. Incidental adrenal lesions: Principles, techniques, and algorithms for imaging characterization. Radiology 2008;249:756-75.
27. Slattery JM, Blake MA, Kalra MK, Misdraji J, Sweeney AT, Copeland PM, *et al*. Adrenocortical carcinoma: Contrast washout characteristics on CT. Am J Roentgenol 2006;187:W21-4.
28. Brix D, Allolio B, Fenske W, Agha A, Dralle H, Jurowich C, *et al*. Laparoscopic versus open adrenalectomy for adrenocortical carcinoma: Surgical and oncologic outcome in 152 patients. Eur Urol 2010;58:609-15.
29. Leboulleux S, Deandreis D, Al Ghuzlan A, Aupérin A, Goéré D, Dromain C, *et al*. Adrenocortical carcinoma: Is the surgical approach a risk factor of peritoneal carcinomatosis? Eur J Endocrinol 2010;162:1147-53.
30. Miller BS, Gauger PG, Hammer GD, Doherty GM. Resection of adrenocortical carcinoma is less complete and local recurrence occurs sooner and more often after laparoscopic adrenalectomy than after open adrenalectomy. Surgery 2012;152:1150-7.
31. Bharwani N, Rockall AG, Sahdev A, Gueorguiev M, Drake W, Grossman AB, *et al*. Adrenocortical carcinoma: The range of appearances on CT and MRI. Am J Roentgenol 2011;196:W706-14.
32. Elsayes KM, Mukundan G, Narra VR, Lewis JS Jr, Shirkhoda A, Farooki A, *et al*. Adrenal masses: MR imaging features with pathologic correlation. Radiographics 2004;24 Suppl 1:S73-86.
33. Schlund JF, Kenney PJ, Brown ED, Ascher SM, Brown JJ, Semelka RC. Adrenocortical carcinoma: MR imaging appearance with current techniques. J Magn Reson Imaging 1995;5:171-4.

34. Simhan J, Canter D, Teper E, Smaldone MC, Patil N, Patchefsky A, *et al*. Adrenocortical carcinoma masquerading as a benign adenoma on computed tomography washout study. Urology 2012;79:E19-20.
35. Maghrabi A, Yaqub A, Denning KL, Benhamed N, Faiz S, Saleem T. Challenges in the diagnostic work-up and management of patients with subclinical Cushing's syndrome and bilateral adrenal masses. Endocr Pract 2013;19:515-21.
36. Lattin GE, Sturgill ED, Tujo CA, Marko J, Sanchez-Maldonado KW, Craig WD, *et al*. From the radiologic pathology archives: Adrenal tumors and tumor-like conditions in the adult: Radiologic-pathologic correlation. Radiographics 2014;34:805-29.
37. Khan M, Caoili EM, Davenport MS, Poznanski A, Francis IR, Giordano T, *et al*. CT imaging characteristics of oncocytic adrenal neoplasms (OANs): Comparison with adrenocortical carcinomas. Abdom Imaging 2014;39:86-91.
38. Tirkes T, Gokaslan T, McCrea J, Sandrasegaran K, Hollar MA, Akisik F, *et al*. Oncocytic neoplasms of the adrenal gland. Am J Roentgenol 2011;196:592-6.
39. Kawashima A, Sandler CM, Fishman EK, Charnsangavej C, Yasumori K, Honda H, *et al*. Spectrum of CT findings in nonmalignant disease of the adrenal gland. Radiographics 1998;18:393-412.

Cite this article as: Panda A, Das CJ, Dhamija E, Kumar R, Gupta AK. Adrenal imaging (Part 1): Imaging techniques and primary cortical lesions. Indian J Endocr Metab 2015;19:8-15.

Source of Support: Nil, **Conflict of Interest:** None declared.